Computing the flow past a cylinder with hemispherical ends

G. J. Sheard[*]   M. C. Thompson[*]   K. Hourigan[*]

(Received 18 October 2004, revised 18 November 2005)

Abstract

A novel application of a spectral element method with a Fourier expansion in the third dimension is used to compute the flow past a cylinder with hemispherical ends. This cylinder is useful as it is a sphere at the small length ratio limit, while approaching a straight circular cylinder as the length ratio is increased. Measurements of the Strouhal frequency and mean drag are presented, and results of a grid independence study show that 128 Fourier planes were required to resolve the flow to an accuracy better than 1%. With 64 planes, forces were predicted accurate to 2%, but Strouhal frequencies were over predicted by approximately 8%. The measured Strouhal frequencies provide useful benchmark data for future low Reynolds number studies of the flow past short cylinders.

[*]Fluids Laboratory for Aeronautical and Industrial Research, Dept. of Mechanical Engineering, Monash University, Melbourne, AUSTRALIA.
mailto:Greg.Sheard@eng.monash.edu.au

Contents

1   Introduction

An efficient alternative to the application of three dimensional meshes to model the flow past bodies that contain geometric symmetries [1, 12] is to utilise the symmetry properties of the body to simplify the mesh formulation. Examples of this include the numerous numerical studies that have used the span-wise uniformity of a straight circular cylinder [6, 3, 2] or the azimuthal symmetry of a sphere [22, 21, 20] to model the flow using a two dimensional plane grid, and modeling the variation in flow variables in the third dimension using a Fourier expansion.

This same technique was employed to good result in the determination of the stability properties of the flow past rings [15, 16, 17]. The ring is an example of a body that varies smoothly from a sphere towards a straight circular cylinder as a geometric parameter is varied. A circular cylinder with
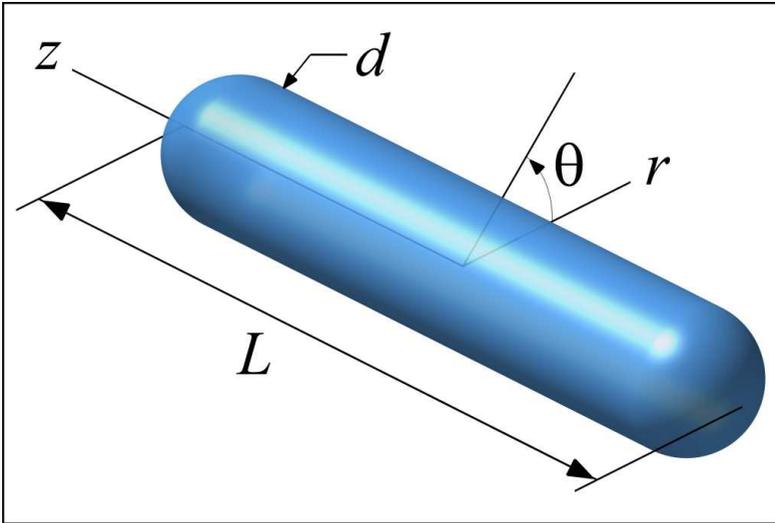
FIGURE 1: The coordinate system relative to a cylinder with hemispherical ends. The direction of flow is in the planes of constant z.

hemispherical ends is another such body, and has been the subject of recent experimental studies [13, 11] aimed at exploiting this property in the study of circular cylinders with small aspect ratios [8, 7]. This geometry is the subject of the present study, in which the flows are numerically simulated. The geometry is described by a length ratio parameter $L_R = L/d$, where L is the length of the cylinder, and d the diameter, and a cylindrical-polar coordinate system is used, with the z-axis coincident with the cylinder axis as shown in Figure 1.

The Reynolds number ($\mathrm{Re} = Ud/\nu$) range of interest in this study is $\mathrm{Re} \lesssim 300$, where U is the free-stream velocity, d is the cross-section diameter of the cylinder, and ν is the kinematic viscosity of the fluid. This range encompasses the transitions to unsteady and three dimensional flows in the wakes behind both spheres and circular cylinders.

A cylinder with hemispherical ends differs from the aforementioned bodies

in that the symmetry axis of the body is normal to the direction of flow rather than parallel. The details of the numerical treatment of this body is discussed in the section to follow.

2 Numerical methodology

This study employs the same spectral element code used previously to compute the three dimensional flow past circular cylinders [19], spheres [20] and rings [17].

For details regarding the spatial discretisation and temporal integration employed as part of the numerical scheme, see [9, 22, 5]. In brief, the computational domain in an rz-plane of symmetry was discretised using quadrilateral spectral elements, which were concentrated in regions where high spatial gradients in velocity and pressure were anticipated (that is, downstream and in the vicinity of the cylinder). Azimuthal discretisation was performed using a Fourier expansion, with P Fourier planes evenly distributed around the cylinder. The even distribution meant that a high number of these planes was required to resolve the wake. Within each element, high order Lagrangian tensor product polynomial basis functions were employed (with N interpolation points in each dimension), and integration over the computational domain was based on a Galerkin finite element method. An example of the mesh employed is shown in Figure 2.

Temporal integration of the incompressible Navier–Stokes equations was carried out using a three step operator splitting scheme, whereby the nonlinear advection step, and the pressure and diffusion steps were computed consecutively. The advection term was integrated using an explicit 3rd order Adams–Bashforth scheme. The pressure term was solved by projecting the intermediate velocity field onto a divergence free space (satisfying the continuity constraint), and solving the resulting Poisson equation. The diffusion term was solved using an implicit 2nd order Crank–Nicolson scheme.
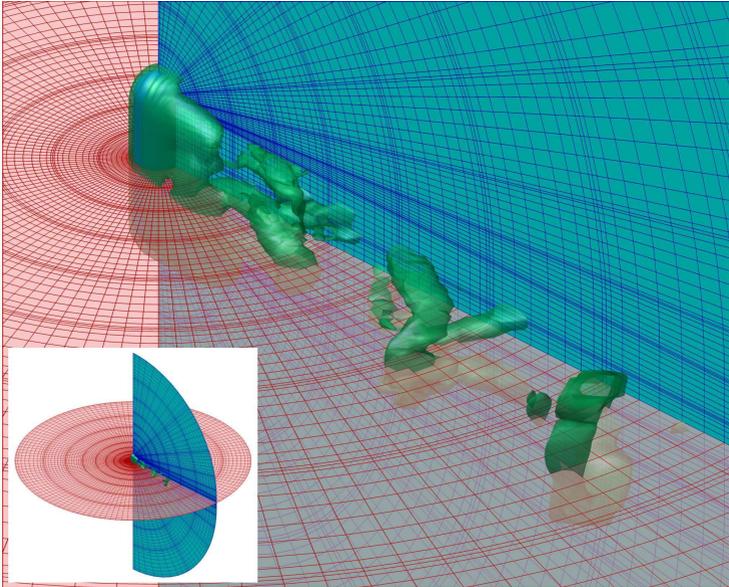
FIGURE 2: The computational mesh employed to discretise the cylinders in this study. Representative computed wake structures are overlaid (green iso-surfaces), the spectral element mesh plane (blue) and a slice through the Fourier expansion (red) are shown, and the interpolation points within each spectral element are visible. Inset: The entire computational domain.

2.1   Geometry specific treatment

In order to resolve the flow normal to a cylinder, a high number of Fourier planes are required. This imposes a restriction on the time step due to the Courant condition, as the spatial wavelength of the Fourier modes are proportional to r, and hence approach zero as $r \to 0$. A filter was applied to eliminate Fourier modes higher than the first mode as the radial distance decreased from $r = 1$ to $r = 0$, which successfully mitigated this problem. Time steps between $0.004 \leq dt \leq 0.005$ were able to be employed, depending on the Reynolds number.

To maximise the computational efficiency of the study, the first task was to determine the optimum number of elements and Fourier planes for the computations. Tests were performed on a sphere modeled using the present "crossflow" flow direction, and these were compared to numerical studies of a sphere that employed a traditional axial flow method [20, 17].

2.2   Comparison of methods for the flow past a sphere

The element distribution over the rz-plane followed closely to past numerical studies for similar Reynolds number ranges [2, 17, e.g.]. Elements were concentrated close to the cylinder surface to resolve the boundary layer, and over the domain downstream of the cylinder to capture the axial variation in the wake.

Figure 3 shows the convergence of global flow quantities with an increase in the number of polynomial interpolation points within each element (N^2). The results are compared to a highly resolved computation with flow in an axial direction from [17]. The figure shows that only the computations with $P = 128$ Fourier planes exhibited convergence of the Strouhal number parameter, indicating that $P = 64$ planes provided insufficient spatial resolution across the wake. Due to the exhaustive requirements of these computations,
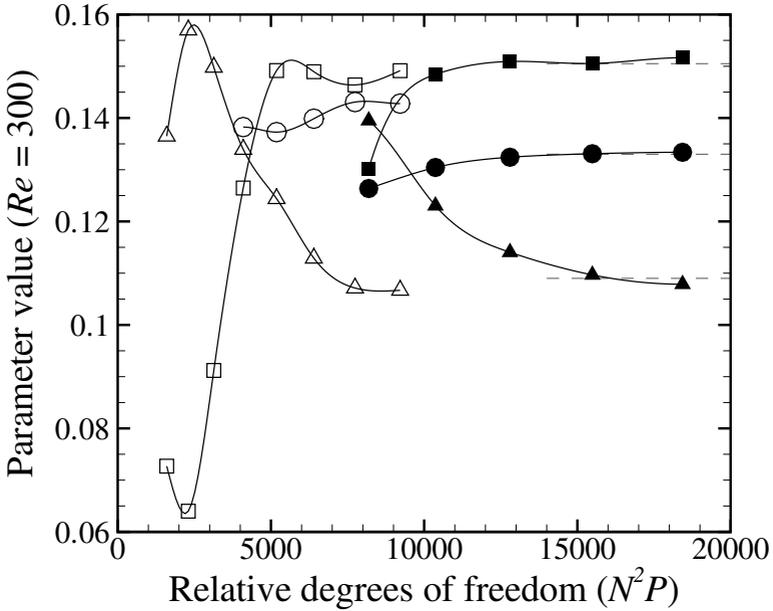
FIGURE 3: Convergence of global flow quantities for a sphere ($L_R = 1$) at Re = 300 with increasing resolution (N^2P). Meshes with $P = 64$ and 128 planes (open and filled symbols, respectively) are shown, and quantities C_{D_p} ($\square$), C_{D_ν} ($\triangle$) and St ($\bigcirc$) are monitored. The dotted lines show accurate values from an axial flow computation [17].
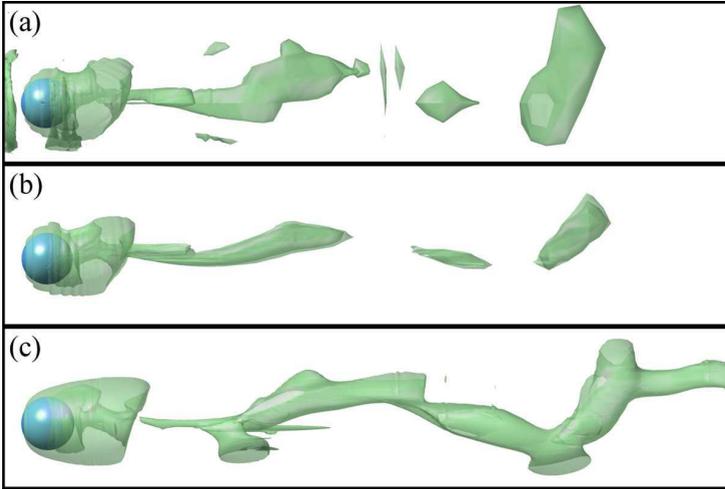
FIGURE 4: A comparison between the crossflow computations with 64 (a) and 128 (b) planes and an accurate axial flow computation (c) for the flow past a sphere at Re = 300. The wakes are shown at similar times during the shedding cycle. Flow is from left to right, and the translucent iso-surface shows the vortical structure of the wake.

the optimum trade off between accuracy and CPU time was determined to be when $P = 128$ planes and $N^2 = 121$ nodes per element were employed, giving an error of less than 2% in terms of both mean drag force and shedding frequency.

The radial trajectory of grid lines away from the cylinder means that resolution drops very rapidly with increasing r. This loss of resolution is apparent from the plots in Figure 4, in which (a) and (b) show the wakes computed using the crossflow grids, and (c) shows an accurate axial flow computation. The under resolved nature of the 64 plane computation is especially evident in Figure 4(a).

The meshes employed in this study typically comprise 100 macro-elements

around the hemispherical ends, plus additional elements along the cylinder span, each containing 121 interpolation points.

3   An axial force oscillation at small length ratios

For cylinders with length ratios $1 \leq L_R \leq 4$, an axial oscillation in the force imparted on the cylinder was detected. A plot of the variation in the Strouhal frequency of this oscillation with length ratio is given in Figure 5. The Strouhal frequency was determined from the peak of the Fourier spectrum recorded over 30 to 50 shedding cycles (peak to peak). For the sphere $(L_R = 1)$ there is no preferred orientation in which unsteady flow develops. The Strouhal frequency for a sphere is included in the plot as it appears to be a natural extrapolation of the St–L_R trend to $L_R = 1$. This implies that the plane in which vorticity is shed from a sphere in the well known hairpin wake [4, 21] is orthogonal to the plane in which the Kármán wake forms behind a circular cylinder. It is therefore expected that the wakes behind cylinders with length ratios $(1 < L_R \ll \infty)$ will exhibit both of these instabilities. For this feature, the upper limit of L_R is yet to be confirmed, but the absence of an axial force component for a cylinder with $L_R = 10$ suggests that the limit could reside within $5 < L_R < 10$.

4   Wake symmetry and shedding frequencies at larger length ratios

Computed mean drag and Strouhal frequency measurements were obtained for a sphere over a range of Reynolds numbers up to Re = 300. These results were in agreement to within 1% of previously reported values. The present
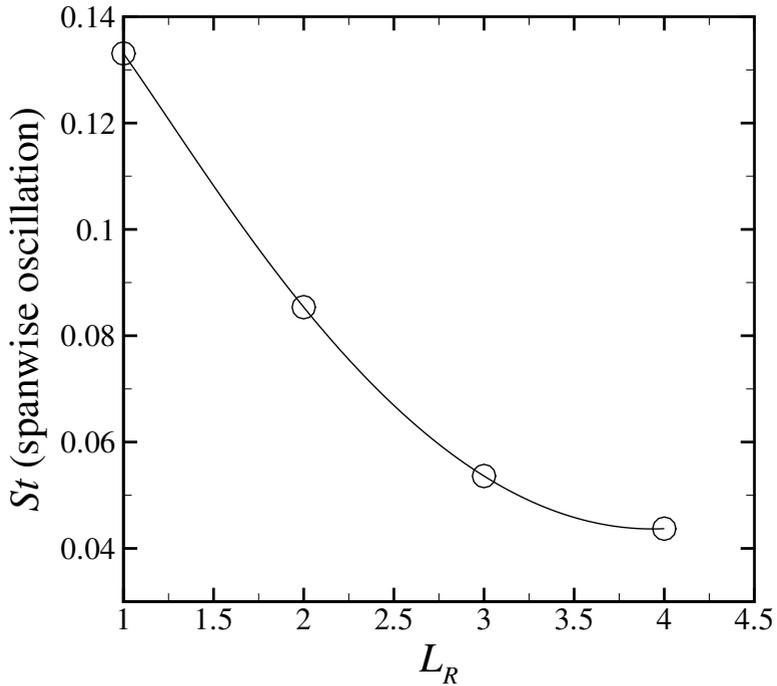
FIGURE 5: A plot of the Strouhal frequency against length ratio for the periodic axial body force oscillation at $\mathrm{Re} = 300$.

study tested cylinders with length ratios $1 \leq L_R \leq 10$. Even with $L_R = 10$, the computed Strouhal–Reynolds number behaviour is very different when compared with a two dimensional circular cylinder, as shown in Figure 6. The plot shows that although the critical Reynolds number for the onset of vortex shedding for this cylinder is within 10–20% of the corresponding value for a straight circular cylinder ($Re_c \approx 47$ [10]), there is a large discrepancy between the trends of the curves beyond the transition. These computations illustrate the significant influence that the three dimensional flow over the hemispherical ends has on the shedding characteristics of the wake. Note that a zero axial force was computed for all Reynolds numbers with $L_R = 10$, whereas cylinders with $1 \leq L_R \leq 5$ all exhibited non-zero axial forcing. Wake symmetry about the cylinder half-span is therefore broken at some length ratio in the range $5 < L_R < 10$. In most cases the axial side forces exhibited a zero mean, but in some cases a non-zero mean was recorded. This topic is pursued further in [18].

5   Concluding remarks and direction for further study

At smaller length ratios ($L_R = L/d \lesssim 5$), the cylinder experiences forcing in both a transverse and an axial direction, suggesting that the flow is not symmetrical about the cylinder mid-point. The flow is symmetrical about the cylinder half-span for cylinders with $L_R \gtrsim 10$.

Further computations are being carried out to determine the nonlinear properties of the first occurring Hopf bifurcations in the wakes of short and long length ratio cylinders.
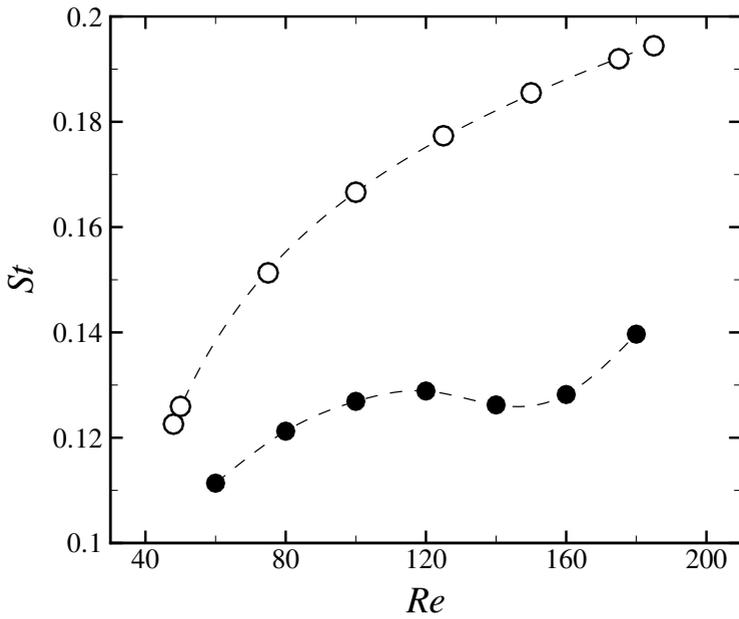
FIGURE 6: Strouhal–Reynolds number profiles for a cylinder with $L_R = 10$ (solid circles), and a straight circular cylinder (open circles) from [14].

References

[1] A. Brydon and M. C. Thompson. Flow interaction between two spheres at moderate Reynolds number. In B. B. Dally, editor, *Proceedings of the Fourteenth Australasian Fluid Mechanics Conference*, pages 693–696, Department of Mechanical Engineering, Adelaide University, S.A. 5005, Australia, 2001. Published by Adelaide University. C1297

[2] R. D. Henderson. Non-linear dynamics and pattern formation in turbulent wake transition. *J. Fluid Mech.*, 352:65–112, 1997. URL C1297, C1301

[3] R. D. Henderson and D. Barkley. Secondary instability in the wake of a circular cylinder. *Phys. Fluids*, 8:1683–1685, 1996. http://dx.doi.org/10.1063/1.868939 C1297

[4] T. A. Johnson and V. C. Patel. Flow past a sphere up to a Reynolds number of 300. *J. Fluid Mech.*, 378:19–70, 1999. URL C1304

[5] G. E. Karniadakis and S. J. Sherwin. *Spectral/*hp *Element Methods for CFD*. Oxford University Press, 1999. C1299

[6] G. E. Karniadakis and G. S. Triantafyllou. Three-dimensional dynamics and transition to turbulence in the wake of bluff objects. *J. Fluid Mech.*, 238:1–30, 1992. URL C1297

[7] N. W. M. Ko, C. W. Law, and K. W. Lo. Mutual interference on transition of wake of circular cylinder. *Phys. Fluids*, 12:1–34, 1962. http://dx.doi.org/10.1063/1.1767109 C1298

[8] C. Norberg. An experimental investigation of the flow around a circular cylinder: Influence of aspect ratio. *J. Fluid Mech.*, 258:287–316, 1994. URL C1298

[9] A. T. Patera. A spectral element method for fluid dynamics: Laminar flow in a channel expansion. *J. Comp. Phys.*, 54:468–488, 1984. http://dx.doi.org/10.1016/0021-9991(84)90128-1 C1299

[10] M. Provansal, C. Mathis, and L. Boyer. Bénard-von Kármán instability: Transient and forced regimes. *J. Fluid Mech.*, 182:1–22, 1987. C1306

[11] M. Provansal, L. Schouveiler, and T. Leweke. From the double vortex street behind a cylinder to the wake of a sphere. *Euro. J. Mech. B (Fluids)*, 23:65–80, 2004. http://dx.doi.org/10.1016/j.euromechflu.2003.09.007 C1298

[12] L. Schouveiler, A. Brydon, T. Leweke, and M. C. Thompson. Interactions of the wakes of two spheres placed side by side. 23:137–145, 2004. http://dx.doi.org/10.1016/j.euromechflu.2003.05.004 C1297

[13] L. Schouveiler and M. Provansal. Periodic wakes of low aspect ratio cylinders with free hemispherical ends. *J. Fluids Struct.*, 14:565–573, 2001. http://dx.doi.org/10.1006/jfls.2000.0351 C1298

[14] G. J. Sheard. *The Stability and Characteristics of the Flow Past Rings.* PhD thesis, Monash University, Melbourne, Australia, 2004. C1307

[15] G. J. Sheard, M. C. Thompson, and K. Hourigan. From spheres to circular cylinders: The stability and flow structures of bluff ring wakes. *J. Fluid Mech.*, 492:147–180, 2003. URL C1297

[16] G. J. Sheard, M. C. Thompson, and K. Hourigan. Asymmetric structure and non-linear transition behaviour of the wakes of toroidal

bodies. *Euro. J. Mech. B (Fluids)*, 23(1):167–179, 2004.
http://dx.doi.org/10.1016/j.euromechflu.2003.04.005 C1297

[17] G. J. Sheard, M. C. Thompson, and K. Hourigan. From spheres to circular cylinders: Non-axisymmetric transitions in the flow past rings. *J. Fluid Mech.*, 506:45–78, 2004. URL C1297, C1299, C1301, C1302

[18] G. J. Sheard, M. C. Thompson, and K. Hourigan. Wake mode development for flow past low aspect ratio cylinders. In K.J. Bathe, editor, *Computational Fluid and Solid Mechanics 2005*, pages 850–853, Massachusetts Institute of Technology, Cambridge MA, USA, 2005. Published by Elsevier. C1306

[19] M. C. Thompson, K. Hourigan, and J. Sheridan. Three-dimensional instabilities in the wake of a circular cylinder. *Exp. Therm. Fluid Sci.*, 12:190–196, 1996.
http://dx.doi.org/10.1016/0894-1777(95)00098-4 C1299

[20] M. C. Thompson, T. Leweke, and M. Provansal. Kinematics and dynamics of sphere wake transition. *J. Fluids Struct.*, 15:575–585, 2001. http://dx.doi.org/10.1006/jfls.2000.0362 C1297, C1299, C1301

[21] A. G. Tomboulides and S. A. Orszag. Numerical investigation of transitional and weak turbulent flow past a sphere. *J. Fluid Mech.*, 416:45–73, 2000. URL C1297, C1304

[22] A. G. Tomboulides, S. A. Orszag, and G. E. Karniadakis. Direct and large-eddy simulation of the flow past a sphere. In *Proceedings of the Second International Conference on Turbulence Modeling and Experiments (2nd ICTME)*, Florence, Italy, 1993. C1297, C1299